PELLETIZED LITHIUM–METAL SULPHIDE CELLS PART I. A SELECTIVE REVIEW

R. W. GLAZEBROOK and M. J. WILLARS

Shell Research Ltd., Thornton Research Centre, P.O. Box 1, Chester CH1 3SH (Gt. Britain)

(Received December 16, 1981; in revised form April 15, 1982)

Summary

One of the most promising advanced battery systems presently under investigation is that based on lithium and sulphur. This review outlines research carried out (mostly over the last decade) in the development of a viable power source. The physical chemistry of the most important materials, notably the aluminium and silicon alloys of lithium and the mono and di-sulphides of iron, is discussed, but the engineering problems associated with high-temperature battery development are not.

---

1. Introduction

Over recent years interest in the use of secondary batteries for transportation and public utility load-levelling has grown. In addition the continued development of solar energy power systems indicates further long-term needs for electricity storage. Unfortunately, the performance and cost of secondary batteries commercially available today severely limit their application in the aforementioned areas.

As a consequence, much attention has recently been focussed upon battery systems of high-energy density (usually containing alkali metal electrodes). One of the most promising systems under investigation is that based on the lithium–sulphur couple, first described in 1969 by the Argonne National Laboratory (ANL) [1].

In its simplest form

$$2Li + S \rightarrow Li_2S \quad E^{\circ}_{300} = 2.25\ V \tag{1}$$

the lithium–sulphur cell has a theoretical energy density of 2625 W h kg^{-1}, which is considerably higher than that of sodium–sulphur (at 1014 W h kg^{-1}), but equally unrealizable in practice.

0378-7753/82/0000-0000/$02.75

Early cells seem to have followed the sodium–sulphur method of construction, but instead of a solid electrolyte, a porous ceramic saturated with lithium chloride/potassium chloride eutectic (m.p. 352 °C) was used, together with a molten sulphur cathode [2].

Failure to produce satisfactory ceramics led to what was effectively a reversal of the component phases, lithium was immobilized in a porous stainless steel mesh (FELTMETAL) and the sulphur was adsorbed on graphite felt, the electrolyte remaining mobile [3]. However, the vapour pressure of sulphur proved to be impractically high and the reaction products, Li_2S_x, too soluble in the electrolyte. Sulphur was next replaced by iron sulphide (FeS, FeS_2 or a mixture of both) and, more recently, lithium has been replaced by lithium–aluminium alloy [4, 5]. Each modification entails a sacrifice of energy density in order to alleviate design difficulties. It is evident also from the literature that these modifications have been necessary to alleviate corrosion problems. Cell operation temperatures are in the range 400 - 500 °C.

Both cylindrical [6] and prismatic [7] lithium–aluminium–iron sulphide cells have been built by Argonne, separation of the active masses generally being achieved by use of a boron nitride cloth.

A much simpler design has been developed at the U.K. Admiralty Marine Technology Establishment (AMTE) as an extension of their work on primary thermal batteries [8]. The cell was assembled from pressed-powder anode, cathode and electrolyte discs, each disc being formulated from active material, electrolyte, and an inert binder which immobilizes the electrolyte (when molten) and serves as an inexpensive electrode separator [9].

The major areas of concern (generally applicable in both pelletized and free-electrolyte designs) in lithium–sulphur technology are discussed in the following sections.

2. Anodes

The difficulty of retention of molten lithium in FELTMETAL, together with the realization of its very corrosive behaviour towards ceramics, led to its early replacement by solid-phase alloys, notably lithium–aluminium and lithium–silicon.

2.1. Lithium–aluminium alloy

Limitations on the use of lithium–aluminium alloys can be best discussed by reference to the phase diagram of Fig. 1. The normally recommended range of useful composition is that represented by the $\alpha + \beta$ two-phase region [10]. Throughout the region the α-phase, lithium-saturated aluminium, is in equilibrium with the vario-stoichiometric intermetallic compound of nominal composition "LiAl"

$$\underset{\alpha\text{-phase}}{Li} + Al \rightleftharpoons \underset{\beta\text{-phase}}{LiAl} \qquad (2)$$

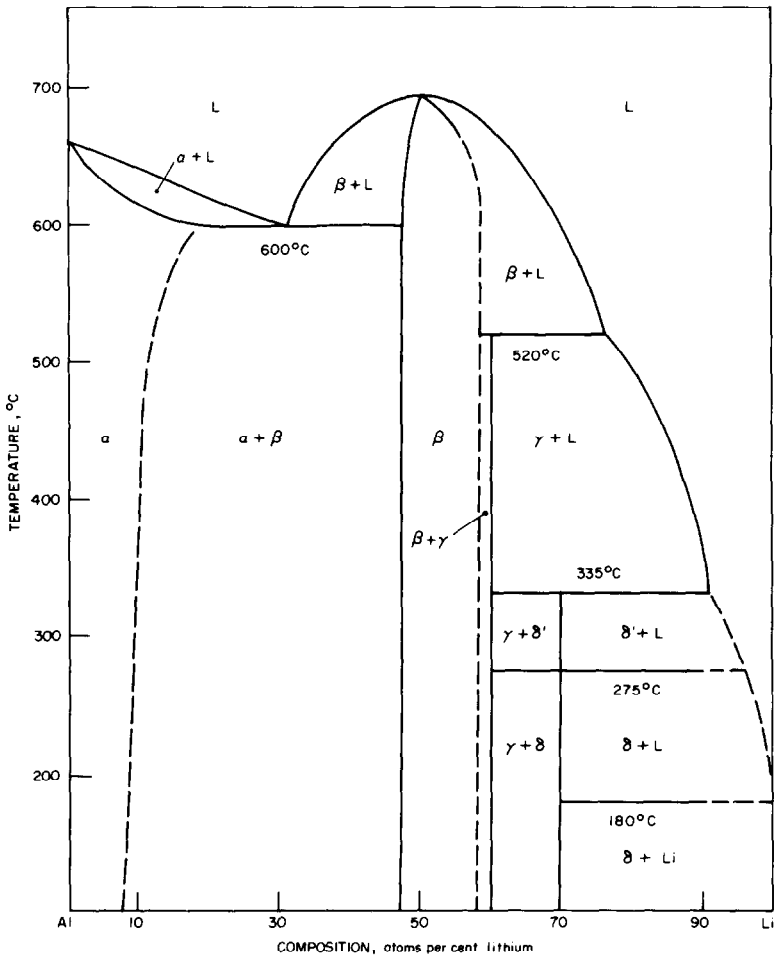

Fig. 1. Phase diagram of the lithium–aluminium alloy system. α, Li-saturated Al; β, LiAl; γ, Li_3Al_2; $\delta = \delta'$, Li_9Al_4.

the relative amounts of the two phases varying as the overall concentration of lithium changes. The lithium activity (and, hence, its electrode potential) remains constant over this region at 300 mV positive to lithium metal. Beyond the β region the potential falls sharply towards that of pure lithium which is undesirable (because of corrosion problems), whilst at the opposite boundary, in the α region, the lithium concentration rapidly diminishes and the potential rises to impractical levels. The useful limits of lithium–aluminium alloy are accordingly between 10 and 48 atoms % [11]. The lower limit is seldom referred to in publications although it is clear from Fig. 2 that some 20% of the lithium present in the alloy is not available for use. It should be noted also that 48 at.% of lithium is only 19% by weight in the alloy.

Several methods have been employed for fabricating lithium–aluminium cathodes [12], *viz.*,

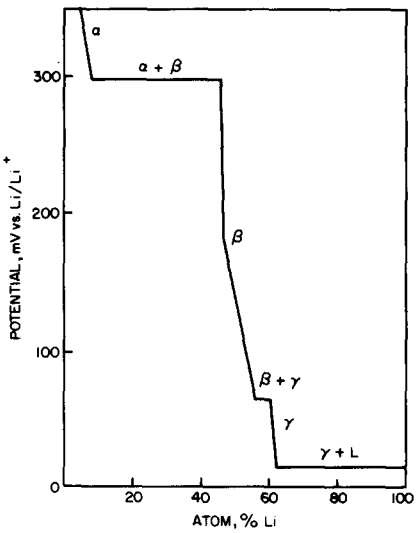

Fig. 2. Potential *vs.* composition for the system LiAl at 423 °C.

(1) electrochemical deposition of lithium from molten electrolyte onto compressed aluminium fibre;

(2) electrochemical deposition onto aluminium powder vibratorily loaded into a porous metal current collector (typically RETIMET, a proprietary porous iron);

(3) powdered pyrometallurgical alloy vibratorily loaded into a porous metal current collector;

(4) hot and cold pressing mixtures of LiCl–KCl electrolyte and powdered pyrometallurgical alloy.

The best results obtained recently [13] (using the latter method) employed electrodes with a loading density of 60 - 70 vol.% in the charged state.

The thicker the electrode the more important it becomes to provide a current collector rather than to rely on the conductivity of the alloy itself. Although initially, cycling may increase electrode capacity, an effect associated with an increase in surface area and with surface defects [14], the general result is a steady decline in capacity. The reason for the capacity decline is not fully understood but it was thought to be due, principally, to a loss of integrity of the alloy structure giving rise to material loss and high interparticle resistance between remaining particles [12]. Recent work [13] however, suggests that the formation of LiAl agglomerates near the centre of the negative electrode may be responsible for the decline.

Marked changes in the morphology of electrode structures have been reported by workers using ternary alloys of LiAl with magnesium [15] or tin, lead, copper or indium [16]. The dendritic form of LiAlIn alloys (yielding a higher surface area) is thought to be responsible for the improved lithium utilization in early cycles [17], but wire electrodes of this material did not retain their integrity. The powdered electrodes produced by Vissers *et al.* [18]

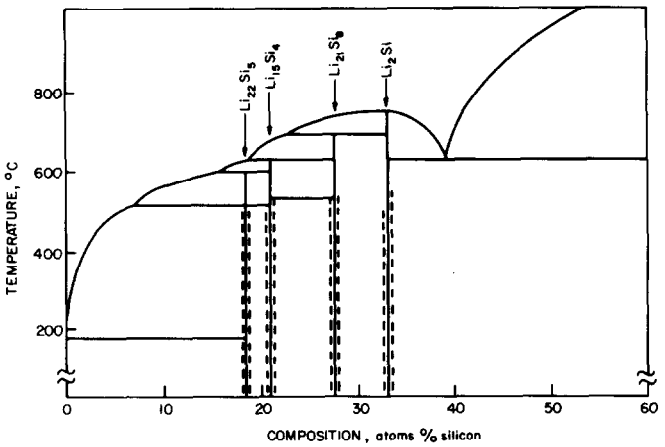

Fig. 3. Phase diagram of the lithium–silicon alloy system.

even so exhibited rates of capacity decline approximately one-sixth (for a 3.9% In alloy) that of LiAl.

2.2. Lithium–silicon alloy

Lithium–silicon alloys are being developed as alternative negative electrode materials [19, 20]. The lithium–silicon phase diagram, Fig. 3, is more complex and less well characterized than that of lithium–aluminium. The useful composition range lies below 83 at.% lithium, corresponding to approximately Li_5Si, and beyond which the chemical activity of lithium is too high. Between 83 at.% and 0% lithium lie four voltage plateaux, Fig. 4, which correspond to the four solid-phase regions to the right in Fig. 3. These regions correspond to non-stoichiometric compounds having compositions variable over fairly narrow limits and giving rise to some uncertainty as to their precise identity. The net effect is that the lithium–silicon anode cycles in voltage steps ranging from 48 mV to 336 mV positive to lithium with an average of 228 mV positive. Multi-voltage steps are not desirable in battery technology but the lithium–silicon alloy has three advantages over lithium–aluminium, *viz.*,

(1) it can be used up to much higher lithium content (*i.e.*, up to 55 wt.%) and therefore has twice the specific capacity [20];

(2) the average electrode potential is lower and therefore it provides a higher cell voltage;

(3) higher power is possible since the diffusion rate of lithium into silicon is higher than into aluminium [21, 22].

Electrodes can be fabricated by filling metallic honeycomb structures of low carbon steel or stainless steel with either the required alloy, *e.g.*, Li_5Si, or with powdered silicon followed by electrochemical charging [20]. Utilization of the latter type proved to be poor until an unspecified proprietary additive was added to the silicon powder. In these circumstances electrochemically formed electrodes are preferred, yielding between 75 and 99%

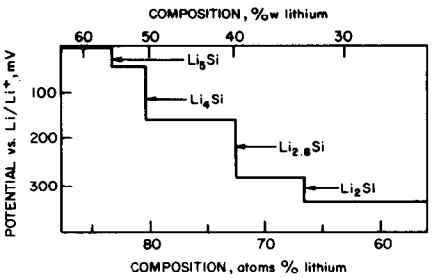

Fig. 4. Potential *vs.* composition for the system LiSi at 400 °C.

utilization depending on current density. Current efficiencies are invariably in the region of 95%.

A major disadvantage of the lithium–silicon alloy is that silicon reacts with steel current collectors causing embrittlement and ultimately breakdown of the electrode structure. Remedies include the use of titanium mesh or titanium-plated metals or the use of yet further additives in the alloy [20, 23].

3. Cathodes

The use of elemental sulphur, like that of lithium, proved to be impractical in early cells for the following reasons:

(1) the high vapour pressure at cell temperature permits transport of sulphur to the anode;

(2) electrolyte-soluble polysulphide ions are formed which similarly to (1) are transported to the anode;

(3) liquid sulphur becomes entrained in the electrolyte.

The net result of these processes, of which (2) predominates, is the irreversible formation of Li_2S at the anode [24, 25].

A number of transition metal sulphides (Cu, Cr, Mn, Fe and Ni) have been examined as alternative sources of sulphur at lower activity, iron sulphides being preferred on grounds of cost as well as for the higher energy densities available [26, 27]. Interestingly, it has been reported that nickel sulphide, NiS_2, may also be a useful material because of its superior electrochemical reversibility [28].

Both ferrous sulphide, FeS, and iron disulphide, FeS_2, are used in lithium–sulphur battery programmes. Broadly they may be compared as follows:

(1) Sulphur activity and concentration is highest in FeS_2, which accordingly provides the higher cell voltage and the higher energy density.

(2) FeS_2 is much more corrosive than FeS and containment is more difficult and expensive.

(3) FeS_2 is a better conductor than FeS so that high utilizations (*i.e.*, above 70%) can be retained even in relatively thick electrodes [27].

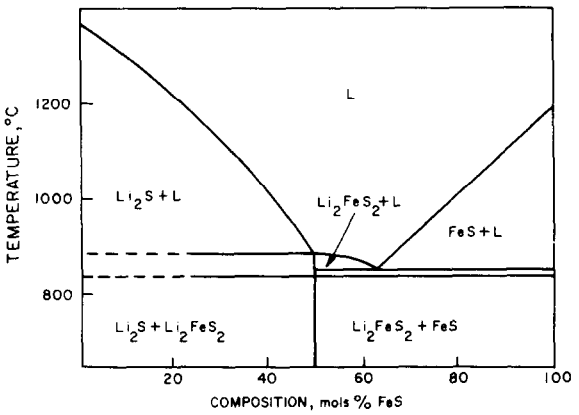

Fig. 5. Phase diagram of the lithium sulphide/ferrous sulphide system.

(4) FeS_2 reduces to Fe on discharge *via* FeS, resulting in a two-plateau voltage charge/discharge characteristic.

A consequence of these properties is that FeS, providing the lower energy density at the lower cost, is more appropriate for use in load-levelling battery design, whereas FeS_2, providing the higher energy and power densities, albeit at higher cost, is more appropriate for use in transportation battery designs.

3.1. Ferrous sulphide (FeS)

The ferrous sulphide cathode discharges at a voltage of approximately 1.6 V *vs.* Li/Li^+. Lithium is transported on discharge to the cathode where it reacts to form insoluble Li_2S. The phase diagram for ferrous sulphide/lithium sulphide, Fig. 5, shows that actually a compound Li_2S:FeS is formed and by extrapolating to temperatures of interest (400 - 450 °C), that two two-phase regions exist [24]. If the ferrous sulphide electrode is cycled in an electrolyte containing only lithium cations good reversibility is obtained [29], so that the formation of Li_2S:FeS (the so called "X phase") is not detrimental. The volume of the cathode in the discharged state is, theoretically, 1.9 times that in the charged state [26] and sufficient pore volume must be provided to allow for this. However, in the normal potassium ion-containing electrolytes there is a reaction between K^+ and the cathode to form a compound (the so-called "J-phase") with a composition approximating to $LiK_6Fe_{24}S_{26}Cl$ [30].

Using a combination of spectroscopic and electrochemical techniques it has been proposed recently [31] that for cells operated at low charge/discharge rates (such that the electrode/electrolyte phases are near to their thermodynamic equilibrium), the predominant reaction sequence is as follows:

$$\underbrace{Li_2S \rightarrow X \rightarrow J \rightarrow FeS}_{\text{charge}} \underbrace{\rightarrow J \rightarrow Li_2S.}_{\text{discharge}}$$

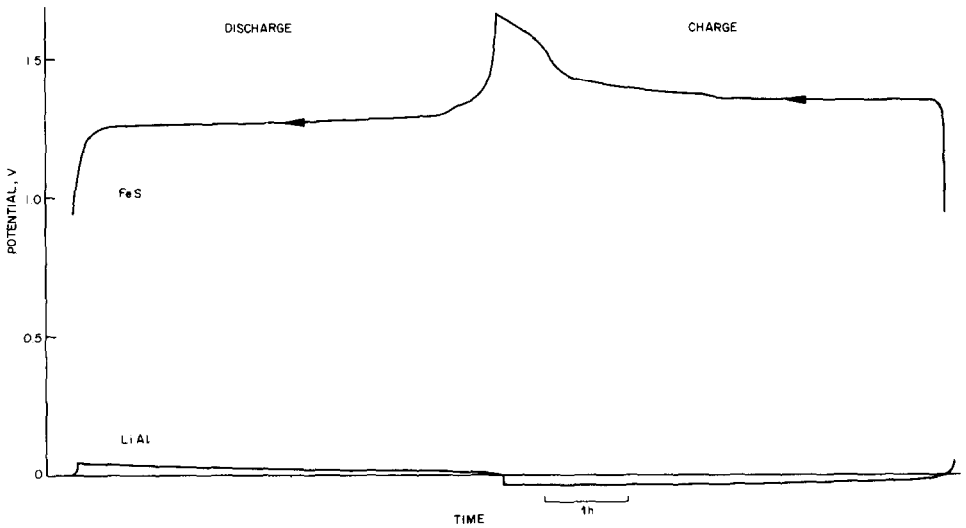

Fig. 6. Charge/discharge cycle for a pelletized LiAl–FeS (i = 12.5 mA cm^{-2}, T = 450 °C), individual electrode potentials monitored w.r.t. LiAl reference.

Indeed, we have shown that for pelletized LiAl–FeS cells cycled in an LiCl–KCl eutectic mixture at 450 °C (Fig. 6), three distinct potential plateaux are apparent on the charging curve (though the discharge process appears less complex). The relative non-reversibility of the J-phase [32] and the unacceptable degree of cathode swelling that accompanies its formation make its suppression very desirable. Methods said to prevent or at least inhibit its formation include the addition of cuprous sulphide [7], operation at higher temperature, and exclusive use of lithium salts as electrolyte [29]. The preferred method, addition of cuprous sulphide, is not problem-free since Cu_2S is noticeably soluble in the electrolyte, reduces at the anode on discharge and may cause cell failure by metallic copper short-circuiting [33].

The conductivity of ferrous sulphide is rather low and even though conductivity additives (notably carbon or graphite) are usually added, high utilization can be achieved only at relatively low current densities (*e.g.*, 70% at 50 mA cm^{-2}). In consequence, practicable electrode thicknesses range from 0.5 to 1.0 cm [27]. This means that relatively large areas of separator materials are required. These are expensive materials in most current cell designs. On the other hand, ferrous sulphide is not nearly as corrosive as iron disulphide (FeS_2) towards metals and the cell recharging voltage is much lower (*viz.*, approximately 1.6 V). Consequently ferrous sulphide cathodes can be utilized with iron current collectors and iron or stainless steel containers, although some corrosion still occurs [34].

3.2. Iron disulphide (FeS_2)

The iron disulphide cathode exhibits a characteristic two-level voltage curve, the lower level at approximately 1.6 V and the upper at approximately

2.0 V [35]. Cyclic voltammetric studies show that the lower level plateau (corresponding broadly to FeS) is electrochemically reversible whereas the upper level is not, indicating that whereas reduction of iron disulphide occurs readily enough, re-oxidation is difficult [34]. Solid-state studies show that in addition to Li_2S:FeS (the "X-phase" as found in FeS cathodes) a possible compound $Li_3Fe_2S_4$ ("Z-phase") is formed, as well as traces of the "J-phase" more generally associated with FeS cathodes [36]. For no clear reason the J-phase does not form so readily, or at least is easily avoided, in iron disulphide cathodes. It appears that the X-phase is formed at voltages below 1.95 V *vs.* Li/Li^+, the Z-phase, together with ferrous sulphide (pyrrhotite, $Fe_{1-x}S$) at 1.95 - 2.15 V, and the Z-phase plus ferrous sulphide and iron disulphide at between 2.15 and 2.25 V. It is generally difficult to return to the fully charged state [37]. Only above 2.5 V will iron disulphide be reformed completely. The recharge voltage is critical because any overcharge voltage will result in the formation of ferrous chloride and free sulphur by reaction of iron disulphide with chloride ion from the electrolyte. The commonly stated opinion that cathode swelling is more controllable in iron disulphide than in ferrous sulphide electrodes [38] is associated with the absence of the J-phase, although the theoretical volumetric ratio of the discharged/charged electrode is 2.6/1 [26] and at the very least this change must be allowed for in electrode design. The addition of cobalt sulphide, CoS_2, to iron disulphide electrodes, although said to alleviate swelling problems, is primarily made to improve the specific conductivity and the lithium diffusion rate within the solid and so promote better utilization [38, 39].

The addition of cobalt sulphide to the iron disulphide cathode is not sufficient to provide adequate conductivity by itself, and a conducting component such as graphite or a metal is always added. Unfortunately, iron disulphide is itself very corrosive towards metals, and near the end of recharge high-activity sulphur species can form which aggravate the situation. To-date, only graphite, molybdenum and tungsten have been shown to have acceptable corrosion resistance [26]. Stainless steel, nickel and other such materials, although often used experimentally, are quite unsatisfactory. Hastelloy B (a Ni/Mo/Fe/Cr alloy) is said to be marginally resistant [26]. Current collectors and containers based on "cheap" iron or stainless steel, plated with the borides, nitrides or carbides of titanium, tantalum, niobium or vanadium, are being evaluated. Best results have been achieved with TiN [40]. Nevertheless, a report from Argonne [41] states that the protection afforded by such coatings in their present forms is insufficient to warrant the large effort that would be required to remedy their defects.

4. Electrolytes

The eutectic mixture of lithium chloride (58 mol.%) and potassium chloride (42 mol.%) melting at 352 °C (Fig. 7) is commonly used, and sets the

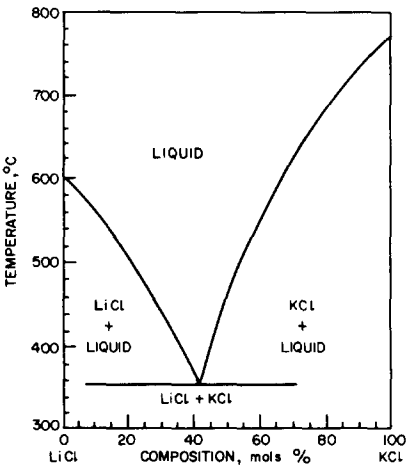

Fig. 7. Phase diagram of the lithium chloride/potassium chloride system.

lower practical cell temperature at approximately 400 °C. The passage of current *via* lithium ions will inevitably lead to the establishment of composition gradients within the electrolyte which, depending on current density and temperature, can lead to the separation as a solid phase of the locally excess component. Such conditions have been analysed theoretically [42 - 44] and recently shown to limit the capacity of pelletized LiAl–FeS cells operated at high current density [45]. Enrichment of electrolyte by potassium chloride in the neighbourhood of the cathode, which occurs on discharge, is also a primary cause of the formation of the undesirable J-phase. The use of lithium-rich electrolytes can alleviate this particular problem, enabling higher utilization and current densities to be achieved by reducing local electrolyte freezing and the formation of J-phase [42, 46, 47]. From the performance point of view an electrolyte containing exclusively lithium cations would be advantageous. Cells based on lithium fluoride, lithium chloride and lithium iodide/lithium bromide have been tested and said to yield higher performance. However, the cost of iodide and bromide electrolytes is apparently unacceptably high [38].

5. Separators

The active materials in present designs of lithium–sulphur cells although solid, are in particulate form and must be separated by an electrolyte-permeable barrier. The requirements of suitable porosity, stability, thickness, etc., are more difficult to meet in these cells because of the high temperature and more corrosive environment.

The only ceramic materials that are compatible with molten lithium (or LiAl alloy) are those which are more stable than the corresponding lithium

compounds, and their corrosion resistance is an extremely sensitive function of the amount and distribution of impurities. A useful review of the properties of a range of ceramic materials of potential use in fused salt cells has been published by Battelle [48]. The following materials have been identified as suitable insulator and separator materials: Y_2O_3, BeO, MgO, BN and AlN.

In pursuit of the desired goal two quite different approaches have been adopted. The first is by the use of woven cloth separators (usually of boron nitride). These materials although satisfactory in themselves are too costly in woven form for commercial batteries and attempts are being made, with some degree of success, to develop cheaper forms such as felts and papers [49 - 51].

The second method is by the use of paste electrolytes which provide electrolyte immobilization and mechanical strength [51, 52]. The paste is formed simply by adding the appropriate amount of fine particle inert filler to the electrolyte mixture. Cells fabricated in this way have exhibited remarkable cycle lifetimes (> 2000 charge/discharge cycles) [53]. Magnesia is particularly attractive [54, 55] because of its low cost, and appears to have adequate stability if sufficiently pure [36].

6. Conclusions

Most of the work to-date concerning lithium–sulphur batteries has concentrated on the aluminium and silicon alloys of lithium in conjunction with iron sulphide.

Lithium–silicon alloys enable cells of higher energy and power density to be constructed but the potential profile on discharge is multi-stepped in contrast to that of Li–Al. Likewise, FeS_2 offers an advantage with respect to sulphur activity, but is far more corrosive than FeS and has a two-plateau discharge characteristic.

Most of the data have been collected in lithium chloride–potassium chloride electrolytes which are susceptible to phase separation phenomena at high rates of discharge and which may encourage the formation of undesirable phases within the FeS electrode leading to considerable shape changes. These effects appear less significant in flooded systems and may be overcome if all-lithium-salt-electrolytes were adopted but a high cost penalty would be incurred.

For many years electrode separation has been achieved by the employment of woven ceramic fabrics but owing to their relatively high cost and the inherent complexity of cell construction, there is increasingly a trend towards the adoption of powder separators.

References

1 E. J. Cairns and H. Shimotake, *Science, 164* (1969) 1347.
2 E. J. Cairns *et al.*, *Argonne Nat. Lab. Rep. ANL-7888*, 1971, and *ANL-7953*, 1972.

3 E. C. Gay, R. K. Steunenberg, J. E. Battles and E. J. Cairns, *8th IECEC*, Philadelphia (1973) *paper 739033*.
4 E. C. Gay, W. W. Schertz, F. J. Martino and K. E. Anderson, *9th IECEC*, San Francisco (1974) *paper 749122*.
5 W. J. Walsh, J. W. Allen, J. D. Arntzen, L. G. Bartholme, H. Shimotake, H. C. Tsai and N. P. Yao, *9th IECEC*, San Francisco (1974) *paper 749140*.
6 W. J. Walsh and H. Shimotake, in D. H. Collins (ed.), *Power Sources 6*, Academic Press, London, 1977, p. 725.
7 E. C. Gay, D. R. Vissers, N. P. Yao, F. J. Martino, T. D. Kaun and Z. Tomczuk, in D. H. Collins (ed.), *Power Sources 6*, Academic Press, London, 1977, p. 735.
8 B. A. Askew and R. Holland, Ext. Abstract, *148th Electrochem. Soc. Meeting*, Dallas (October 1975) paper *27*, *75* (2).
9 D. Birt, C. Feltham, G. Hazzard and L. Pearce, in J. Thomson (ed.), *Power Sources 7*, Academic Press, London, NewYork and San Francisco, 1979, p. 691.
10 J. R. Selman, D. K. DeNuccio, C. J. Sy and R. K. Steunenberg, *J. Electrochem. Soc.*, *124* (1977) 1160.
11 C. J. Wen, W. Weppner, B. A. Boukamp and R. A. Huggins, *J. Electrochem. Soc.*, *126* (1979) 2258.
12 See, for example: E. C. Gay, D. R. Vissers, F. J. Martino and K. E. Anderson, *J. Electrochem. Soc.*, *123* (1976) 1591; D. R. Vissers and K. E. Anderson, *Argonne Nat. Lab. Rep. ANL-76-8*, 1976, p. B176.
13 D. L. Barney *et al.*, *Argonne Nat. Lab. Rep. ANL-79-94*, 1980.
14 C. A. Melendres and C. C. Sy, *J. Electrochem. Soc.*, *125* (1978) 727.
15 C. A. Melendres, S. Siegel and J. Settle, *J. Electrochem. Soc.*, *125* (1978) 1886.
16 D. R. Vissers, K. E. Anderson and W. R. Frost, Ext. Abstract, *150th Electrochem. Soc. Meeting, Las Vegas, October, 1976*, p. 115.
17 W. Cheng, *J. Electrochem. Soc.*, *126* (1979) 483C.
18 D. R. Vissers, K. E. Anderson and F. C. Mrazek, *Argonne Nat. Lab. Rep. CONF 770531-4*, 1977.
19 R. A. Sharma and R. N. Seefurth, *J. Electrochem. Soc.*, *123* (1976) 1763.
20 See, for example: S. Lai, *J. Electrochem. Soc.*, *123* (1976) 1196; S. Lai and A. F. Samells, *12th IECEC*, Washington D.C. (1977) *paper 779062*.
21 See, for example: H. -G.v. Schnering, R. Nesper, K. Tebbe and J. Curda, *Z. Metallk.*, *71* (1980) 357; C. J. Wen and R. A. Huggins, *J. Solid State Chem.*, *37* (1981) 271.
22 See, for example: R. N. Seefurth and R. A. Sharma, *J. Electrochem. Soc.*, *124* (1977) 1207; E. N. Protasov, A. A. Gnilomedov, A. L. L'vov, A. A. Suchkov and A. S. Ivanov, *Elektrokhimiya*, *17* (1981) 913.
23 S. Sudar, L. A. Heredy, J. C. Hall and L. R. McCoy, *12th IECEC*, Washington D.C. (1977) *paper 779061*.
24 R. A. Sharma, *J. Electrochem. Soc.*, *123* (1976) 448.
25 Z. Tomczuk, R. E. Hollins and R. K. Steunenberg, *Argonne Nat. Lab. Rep. ANL-76-8*, 1976, B99.
26 S. Sudar, L. R. McCoy and L. A. Heredy, *10th IECEC*, Newark (1975) *paper 759099*.
27 P. A. Nelson *et al.*, *Argonne Nat. Lab. Rep. ANL-75-20*, 1975.
28 S. K. Preto, S. von Winbush and M. F. Roche, *J. Electrochem. Soc.*, *125* (1978) 369C.
29 H. Shimotake and L. G. Bartholme, *Argonne Nat. Lab. Rep. ANL-76-8*, 1976, B210.
30 M. L. Saboungi, J. J. Marr and M. Blander, *J. Electrochem. Soc.*, *125* (1978) 1567.
31 Z. Tomczuk, S. K. Preto and M. F. Roche, *J. Electrochem. Soc.*, *128* (1981) 760.
32 K. W. Kam and K. E. Johnson, *J. Electroanal. Chem.*, *115* (1980) 53.
33 J. E. Battles and F. C. Mrazek, Ext. Abstract, *152nd Meeting Electrochem. Soc., Atlanta, October, 1977*, 77-2, 161.
34 P. A. Nelson *et al.*, *Argonne Nat. Lab. Rep. ANL-76-45*, 1976.
35 D. R. Vissers, Z. Tomczuk and R. K. Steunenberg, *J. Electrochem. Soc.*, *121* (1974) 665.
36 P. A. Nelson *et al.*, *Argonne Nat. Lab. Rep. ANL-77-68*, 1977.

37 E. J. Cairns and J. S. Dunning, *Argonne Nat. Lab. Rep. ANL-76-8*, 1976, A81.
38 H. Shimotake, W. J. Walsh, E. S. Carr and L. G. Bartholme, *11th IECEC*, State Line (1976) *paper 769080*.
39 C. C. McPheeters, W. W. Schertz and N. P. Yao, Ext. Abstract, *148th Meeting Electrochem. Soc.*, Dallas (October 1975), p. 70.
40 N. Koura, J. E. Kincinas and N. P. Yao, Ext. Abstract, *148th Meeting Electrochem. Soc.*, Dallas (October 1975), p. 81.
41 K. M. Myles, F. C. Mrazek, J. A. Smaga and J. L. Settle, *Argonne Nat. Lab. Rep. ANL-76-8*, 1976, B50.
42 C. E. Vallet and J. Braunstein, *J. Electrochem. Soc., 125* (1978) 1193.
43 J. Braunstein and C. E. Vallet, *J. Electrochem. Soc., 126* (1979) 960.
44 C. E. Vallet, D. E. Heatherly and J. Braunstein, *J. Electrochem. Soc., 127* (1980) 1.
45 M. J. Willars, J. G. Smith and R. W. Glazebrook, *J. Appl. Electrochem., 11* (1981) 335.
46 D. R. Vissers, K. E. Anderson, C. K. Ho and H. Shimotake, *J. Electrochem. Soc., 125* (1978) 335C, Abstract no. 34.
47 F. J. Martino, L. G. Bartholme, E. C. Gray and H. Shimotake, *J. Electrochem. Soc., 125* (1978) 335C, Abstract no. 35.
48 E. W. Brooman, K. R. Shillito and W. D. Boyd, *Battelle Rep. AD A044888*, 1977.
49 P. A. Nelson *et al.*, *Argonne Nat. Lab. Rep. ANL-76-98*, 1976.
50 J. P. Mathers, T. W. Olszanski and J. E. Battles, *J. Electrochem. Soc., 124* (1977) 1149.
51 R. D. Walker, C. C. Cheng, J. E. Battles and J. P. Mathers, *Argonne Nat. Lab. Rep. ANL-76-8*, 1976, B41.
52 *U.K. Patent 1,510,642* (1978).
53 D. Birt, C. Feltham, G. Hazzard and L. Pearce, *Proc. 28th Power Sources Symp., Atlantic City, 1978*, p. 14.
54 R. K. Quinn, D. F. Zurawski and N. R. Armstrong, in J. Thompson (ed.), *Power Sources 8*, Academic Press, London, New York and San Francisco, 1981, p. 305.
55 B. A. Askew, P. V. Dand, L. W. Eaton, T. W. Olszanski and E. J. Chaney, in J. Thomson (ed.), *Power Sources 8*, Academic Press, London, New York and San Francisco, 1981, p. 337.